Rapid Spreading of a Droplet on a Thin Soap Film

Motaghian, M.; Shirsavar, R.; Erfanifam, M.; Sabouhi, M.; Van Der Linden, E.; Stone, H.A.; Bonn, D.; Habibi, M.

LANGMUIR

Article

Rapid Spreading of a Droplet on a Thin Soap Film

M. Motaghian,[†] R. Shirsavar,[‡] M. Erfanifam,[‡] M. Sabouhi,[‡] E. van der Linden,[†] H. A. Stone,[§] D. Bonn,[∥] and Mehdi Habibi*[†]

[†]Physics and Physical Chemistry of Foods, Wageningen University, Wageningen 6708 PB, Gelderland, The Netherlands

[‡]Department of Physics, Faculty of Science, University of Zanjan, Zanjan 45371-38791, Zanjan, Iran

[§]Department of Mechanical and Aerospace Engineering, Princeton University, Princeton, New Jersey 08544, United States

[∥]Institute of Physics, van der Waals-Zeeman Institute, University of Amsterdam, Science Park 904, Amsterdam 1098 XH, North Holland, The Netherlands

Ⓢ Supporting Information

ABSTRACT: We study the spreading of a droplet of surfactant solution on a thin suspended soap film as a function of dynamic surface tension and volume of the droplet. Radial growth of the leading edge (R) shows power-law dependence on time with exponents ranging roughly from 0.1 to 1 for different surface tension differences ($\Delta\sigma$) between the film and the droplet. When the surface tension of the droplet is lower than the surface tension of the film ($\Delta\sigma > 0$), we observe rapid spreading of the droplet with $R \approx t^\alpha$, where α ($0.4 < \alpha < 1$) is highly dependent on $\Delta\sigma$. Balance arguments assuming the spreading process is driven by Marangoni stresses versus inertial stresses yield $\alpha = 2/3$. When the surface tension difference does not favor spreading ($\Delta\sigma < 0$), spreading still occurs but is slow with $0.1 < \alpha < 0.2$. This phenomenon could be used for stretching droplets in 2D and modifying thin suspended films.
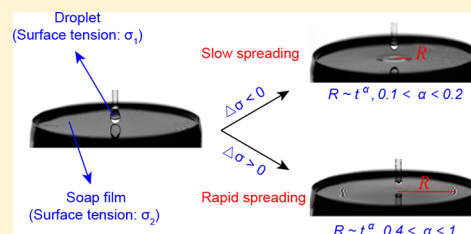
1. INTRODUCTION

The dynamics of the spreading of a droplet over a solid or liquid surface is a phenomenon that has attracted much attention in the past decades.[1,2] Beside its relevance to many fields of technology,[3−5] studying the dynamics of spreading can provide understanding of the various forces acting on an interface.

It has been shown that depositing a droplet on a solid surface will initially result in the formation of a precursor film[6,7] with a molecular thickness,[8] which decreases the spreading rate of the main droplet. However, Fraaije and Cazabat[9] showed that spreading a droplet on a liquid substrate exhibits faster dynamics, and an even faster spreading has been observed in a drop-on-drop geometry.[10] In these previous studies, the radius of the spreading front increases as a function of time according to power law. The exponent of this power-law growth depends on physicochemical properties of both the spreading liquid and the substrate, for example, surface energy, roughness, viscosity,[11] miscibility,[12] immiscibility,[13] and the depth of the substrate for liquid substrates.[9,14,15] When capillary forces are driving the spreading of a drop on a solid substrate and inertial effects are negligible, a balance between viscous forces and capillary forces predicts a slow time evolution of the spreading front, $R \approx t^{1/10}$, known as Tanner's law.[16−18] When two different liquids are brought into contact with each other, it is often the difference in the surface tensions (Marangoni stress) that drives the spreading.[19] For spreading on a thin liquid substrate where the thickness of the film is much smaller than the radius of the spreading front, the lubrication approximation applies. Jensen and Grotberg[20] have

shown that the when viscous effects dominate inertial effects, the width of a planar monolayer strip containing a fixed mass of the surfactant spreads in time as $t^{1/3}$, and the radius of an axisymmetric monolayer droplet evolves as $t^{1/4}$. Numerical studies[21] also confirmed the exponent of 1/4 for spreading of a droplet on a rigid substrate.

Although spreading has been studied under various conditions, spreading a droplet on a soap film of a few micrometers thickness, suspended in air, has not been studied yet to the best of our knowledge. Here, we study a specific case of the droplet spreading on a liquid substrate: we deposit droplets of surfactant solution on a suspended thin soap film and document the spreading dynamics as a function of surface tension and droplet size using high-speed imaging. In contrast to our experimental system, thin liquid substrates studied in previous works[15] were at least a few millimeters thick and in contact with a solid boundary, which causes significant viscous dissipation because of the no-slip boundary condition.

2. EXPERIMENTAL SECTION

To make a horizontal soap film, we used a concentric cylinder made of stainless steel with inner and outer diameters of 39.5 and 40.0 mm, respectively. The concentric cylinder was dipped into sodium dodecyl sulfate (SDS) (Merck) solution to produce a horizontal soap film. Then, a droplet of ammonium lauryl sulfate (ALS) (Fluka) solution or SDS solution was deposited on the soap film using a capillary tube.
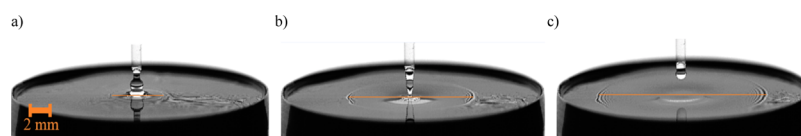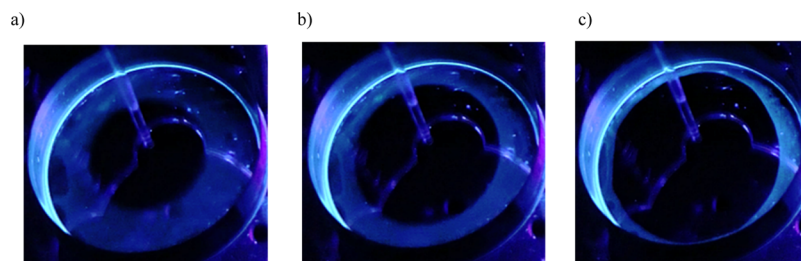
Figure 1. Spreading a droplet of 0.3 M ALS on a soap film of 0.005 M SDS. Images from left to right show the instant of deposition and subsequent stretching of the droplet. From left to right, the images are taken at (a) 5, (b) 12, and (c) 24 ms after deposition.

Figure 2. Spreading of a droplet containing ALS 0.4 M on a soap film of SDS 0.005 M. Fluorescent dye (blue) is added to the initial SDS soap film. From left to right: the droplet (black circle) is stretched toward the edges of the container. Two liquids do not mix during spreading. From left to right, images are taken at (a) 5, (b) 15, and (c) 30 ms after deposition of the droplet.
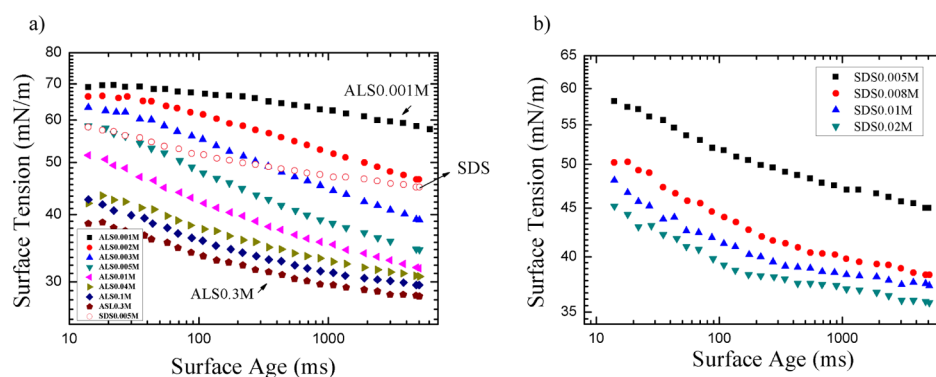
Figure 3. Dynamic surface tension as a function of surface age for (a) different concentrations of ALS solutions and 0.005 M SDS (open symbols) and (b) different concentrations of SDS solutions. Details of the dynamic surface tension measurements are explained in Supporting Information.

The average volume of deposited droplets was 6 ± 0.5 μL, although in one series of experiments, we varied the deposited volume to see how spreading depends on the droplet size. To vary the droplet size, capillary tubes of different diameters were used; for very small droplet sizes, the liquid was sprayed very close to the soap film. SDS solutions with molar concentrations of 0.005 M were used to make the initial soap films, and SDS solutions with concentrations of 0.005, 0.008, 0.01, and 0.02 M and ALS solutions with concentrations of 0.001, 0.002, 0.003, 0.005, 0.01, 0.04, 0.1, and 0.3 M were used for the droplets deposited on the soap film. The critical micelle concentrations (cmc's) of ALS and SDS solutions at 25 °C are 0.0065[22] and 0.0082 M,[23] respectively. For the deposited droplets, the concentrations of solutions corresponded to a range from 0.15 to 46 and 0.6 to 2.4 cmc for ALS and SDS, respectively. Dynamic surface tensions of solutions were measured via the bubble pressure method using a Krüss BP50 bubble surface tensiometer. The thickness of the initial soap film was estimated indirectly from the speed of a traveling mechanical wave on the soap film using the equation for wave speed on an elastic sheet under tension (see Supporting Information). After depositing an ALS droplet, the evolution of the deposited drop on the soap film was recorded using a high-speed camera (Phantom) at a rate of 4000 frames per second. To illuminate the surface of the soap film, we used a white light source with the incident and reflected angles of ~45°. The radius of the leading edge was measured by pixel counting on the frames.

3. RESULTS AND DISCUSSION

We focus on the spreading of a droplet on a suspended liquid film of a few micron thickness. This is different from the other work on Marangoni spreading, where the minimum thickness of liquid substrates[15] was typically about a few millimeters and where the substrates are in contact with a solid boundary. Therefore, we expect the viscous dissipation in our system to be much smaller, which can lead to faster spreading. Furthermore, having a suspended soap film allows us to confine the liquid−liquid interface solely to a circular rim.

To investigate the position of the droplet and the soap film during the course of spreading, we first made qualitative observations. Figure 1 shows an example of spreading a droplet of 0.3 M ALS on a 0.005 M SDS soap film. In Figure 2, spreading of a droplet of ALS 0.4 M on an SDS 0.005 M soap film is shown, in which a fluorescent dye was added to the SDS solution. The sequence of images reveals that, after deposition of the droplet, a nonfluorescent circular film is formed in the center, gradually growing and pushing the fluorescent SDS soap film toward the edge of the container. The absence of fluorescence in the spreading film indicates that the ALS droplet is hardly contaminated by the initial soap film.

This qualitative observation is confirmed by calculating the ratio of advection rate to diffusion rate of our system. This ratio, the Peclet number, is given by $Pe = lu/D$, where l is the

a)

b)
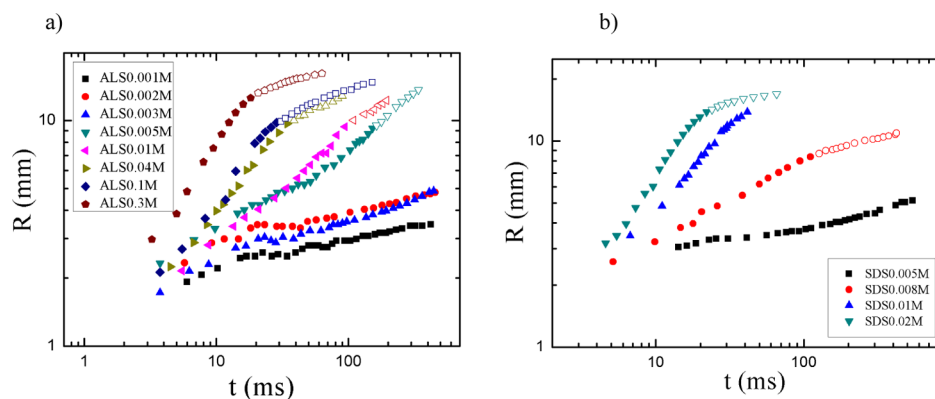
Figure 4. Spreading radius versus time for droplets of ALS (a) and SDS (b) with different concentrations on a soap film of 0.005 M SDS. Open symbols show the cross-over regime because of the boundary effects. Error bars are smaller than the size of the symbols.

a)

b)
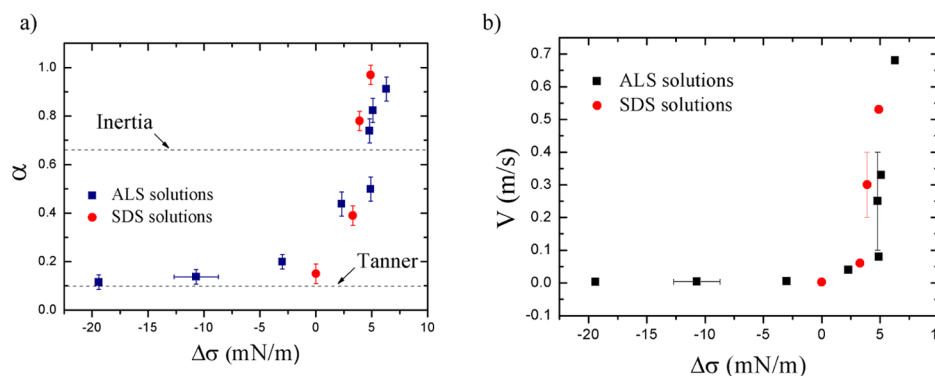
Figure 5. (a) Exponent α as a function of surface tension difference for the deposited droplets with different concentrations of ALS and SDS on the 0.005 M SDS soap film. α is calculated by a power-law fit to data in Figure 4. (b) Average spreading speed calculated by linear fits to the solid data points in Figure 4. For the sake of clarity, only several typical error bars for the velocity and $\Delta\sigma$ are shown.

characteristic length of the system, u is the average flow velocity, and D is the diffusion coefficient. By considering the size of the droplet (~1 mm) as the characteristic length, the lowest spreading speed (~0.1 m/s), and diffusion coefficient of $D \approx 10^{-9}$ m^2 s^{-1} (for a typical surfactant in water[24]), we arrive at a Peclet number significantly greater than 1, confirming that diffusion at the boundaries is negligible during the course of fast spreading.

3.1. Effect of Surface Tension. Figure 3 shows the dynamic surface tension for different concentrations of ALS and SDS as a function of the surface age measured using a bubble pressure surface tensiometer. To determine the effective surface tension difference ($\Delta\sigma$) between the droplets and the soap film in our experiments, we use the time-dependent data of Figure 3. For the ALS droplet, we consider a characteristic time scale given by $\tau = L/u$, where u is the average speed of the spreading film and L is the maximum radius of the spreading film (~1 cm). For the SDS substrate, in each experiment there were at least a few seconds between making the soap film and depositing the ALS droplet; therefore, the surface tension of the SDS at 5 s (Figure 3) is used to calculate $\Delta\sigma$. Taking this into account, the surface tension difference between droplets (ALS) and the soap film (SDS) covers a wide range, from −19.4 mN/m for ALS 0.001 M to 6.3 mN/m for ALS 0.3 M.

In order to identify how surface tension regulates spreading, droplets with different concentrations of ALS and SDS (different surface tensions) were deposited on the soap film containing SDS 0.005 M. After the moment of deposition, the

radius (R) of the leading front was measured as a function of time using high-speed imaging. The results are shown in Figure 4a and b for ALS and SDS droplets spreading on an SDS film, respectively. For the experiments where the radius of the leading front went beyond 1 cm, a cross-over regime is observed (open symbols in Figure 4), probably due to boundary effects (the radius of the cylinder is 2 cm). After discarding the data points at and beyond the cross-over region, a clear power-law behavior for R versus time is observed ($R \propto t^\alpha$). By fitting power-law functions to the closed-symbol data sets, we find exponents α ranging from 0.11 to 0.9 for different surface tension differences (Figure 5a). Power-law growth of spreading fronts has been observed in many other spreading phenomena.[9,12,15,25]

For droplets with low concentrations of ALS, where the surface tension of the droplets is larger than or equal to the surface tension of the soap film ($\Delta\sigma \leq 0$), a slow spreading regime was observed. Here, the surface tension difference is not favorable for the spreading as the new stretched liquid film has a higher surface tension than the original film. For deposited droplets of ALS 0.001, 0.002, and 0.003 M, for which $\Delta\sigma = -19.4$, -10.7, and -3 mN/m, respectively, we obtain power-law exponents of 0.12 ± 0.04, 0.14 ± 0.04, and 0.19 ± 0.04, respectively (Figure 5a).

Figure 6 shows the situation when the droplet and soap film are of the same composition and concentration: SDS 0.005 M. After deposition of the droplet, it forms a lens and spreads slowly (black squares in Figure 4b) with a power-law time dependence and an exponent of 0.15 ± 0.04. This is in contrast
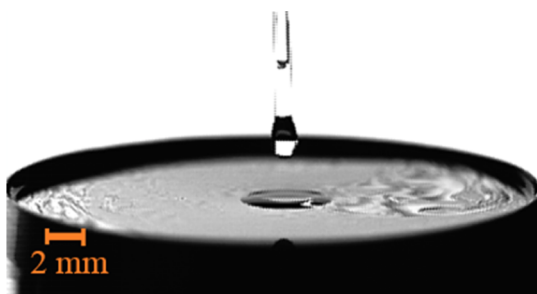
Figure 6. Droplet of 0.005 M SDS is deposited on the same soap film. After deposition, a liquid lens is formed that spreads slowly in time. R as a function of time for this experiment is shown by black squares in Figure 4b.

with an earlier experimental work by Aarts et al.[26] for a three-dimensional configuration where coalescence of two droplets of the same liquid was studied and a linear dependence of radius on time (for early times) was measured, although the current work considers a system with surfactant molecules at the surface and a different surface geometry.

When a drop of SDS spreads slowly on a film of the same liquid ($\Delta\sigma = 0$), there is a clear energetic reason because of lowering the total surface area. This slow spreading with small exponents may be explained by the regime of Tanner's law. In Tanner's regime, the driving force of spreading is because of capillary pressure induced by the curvature at the rim. We note that Tanner's law applies for spreading on a rigid boundary. If the surface exhibits a slip, then, one might expect a slightly different result.[27] We have an almost similar situation for spreading a droplet on the same liquid film, where large curvatures are observed at the rim of the liquid lens. The exponent predicted by Tanner's law is shown by a horizontal dashed line on Figure 5a; it is in agreement with the spreading exponents observed for ($\Delta\sigma = 0$). For droplets with larger surface tension with respect to the film ($\Delta\sigma < 0$), we still see slow spreading dynamics with similar exponents ($\alpha < 0.2$). At first glance, it seems that the spreading should not occur because of higher surface tension of the final film. However, if we consider the very slow dynamics, we can expect that the surface tension difference between the droplet and the film rapidly decreases and reaches a uniform surface tension, which is lower than the original surface tension of the film surface, shortly after the coalescence. In particular, in the slow

spreading regime, the spreading speed is about 1 mm/s, so that it takes several seconds to spread about 1 cm. The data in Figure 3 shows that the surface tension decreases considerably over this time scale, so we anticipate that the surface tension everywhere becomes uniform in the slow spreading regime. Therefore, even in case of $\Delta\sigma < 0$, the slow spreading continues with the Tanner-like dynamics, as discussed above.

For the droplets with lower surface tension than the soap film ($\Delta\sigma > 0$), the exponent α strongly increases with increasing $\Delta\sigma$ (Figure 5a). Here, the positive surface tension difference favors droplet spreading. Because of very fast stretching of the droplet, we expect a gradient of surface tension from the outside film toward the center of the spreading droplet.

We estimate the average spreading speed by fitting a linear function to the data in Figure 4a and b. The results are shown as a function of $\Delta\sigma$ in Figure 5b, ranging from 0.003 m/s for negative $\Delta\sigma$ to about 0.7 m/s for $\Delta\sigma = 6.3$ mN/m. From the average spreading speed, we determine an experimental time scale for the spreading. Using this time scale, we obtain the dynamical surface tensions in Figure 3.

In our system, we observe a range of exponents from $\alpha \approx 0.1$ to linear growth of the front radius ($\alpha \approx 1$). A similar range of spreading exponents was reported previously by Rafaï et al.[28] in a completely different system consisting of a surfactant solution (Trisiloxan) spread on a solid substrate, where by increasing the concentration of surfactant, α increased from 0.2 to 1. This wide range of exponents was associated with Marangoni effects.

3.2. Effect of the Droplet Volume. In order to study the effect of the volume of the droplets on the spreading process, droplets with different diameters (D) were deposited on an SDS 0.005M film. We used ALS 0.04 M droplets for fast spreading and SDS 0.005 M droplets for slow spreading. Figure 7 shows the radius of spreading as a function of time for droplets with different volumes deposited on the soap film. We fit the time-dependencies with a power law and find that the power-law exponent is roughly the same for all droplet volumes in each regime ($\alpha \approx 0.9$ for fast spreading and $\alpha \approx 0.11$ for the slow regime), as shown in Figure 8a. Only for the smallest droplet of ALS, created by spraying, an exponent $\alpha = 0.8 \pm 0.05$ was obtained, which is a little smaller than that of the other experiments in the fast regime. For the fast spreading experiments, because the exponent α is close to unity, we can
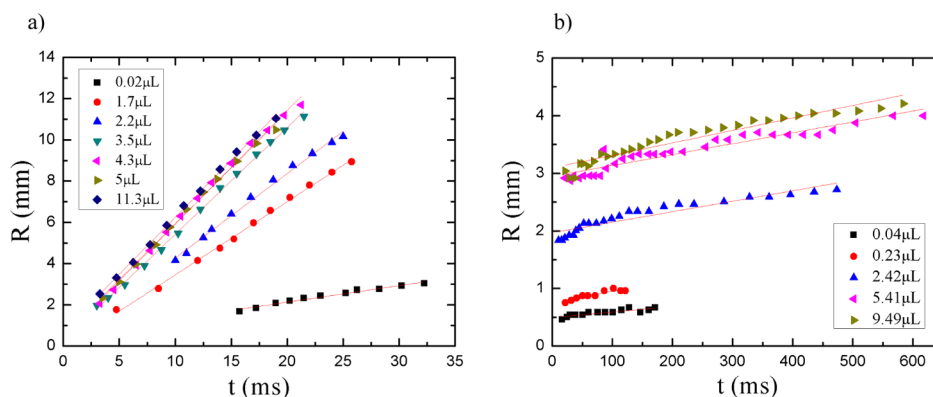
Figure 7. Time evolution of spreading droplets with different volumes on SDS soap films. (a) Spreading of 0.04 M ALS droplets with different volumes (0.02, 1.7, 2.2, 3.5, 4.3, 5, and 11.3 μL) on a 0.005 M SDS soap film (fast spreading). (b) Spreading of 0.005 M SDS droplets with different volumes (0.04, 0.23, 2.42, 5.41, and 9.49 μL) on a 0.005 M SDS soap film (slow spreading). Error bars are smaller than the size of the symbols.
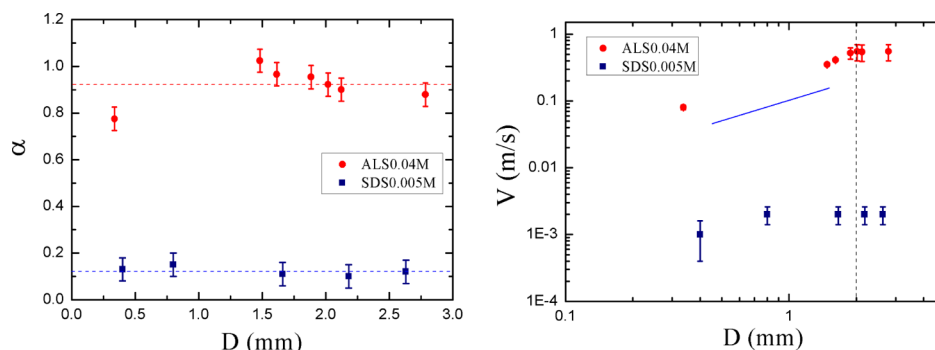
Figure 8. (a) Exponent α calculated by a power-law fit to the data in Figure 7 as a function of the diameter of the droplets (D). Upper and lower horizontal dashed lines represent the average value of α for rapid and slow spreading, respectively. (b) Average spreading speed as a function of the droplet size with logarithmic scales for fast (0.04 M ALS droplet on a soap film of 0.005 M SDS) and slow spreading (0.005 M SDS droplet on 0.005 M SDS soap film). Vertical dashed line illustrates the capillary length of the system. Blue line with slope one is shown as a guide to the eye.

estimate the spreading speed from the slope of linear fits to the data points. In Figure 8b, the spreading speed is reported as a function of the droplet diameter. By increasing the size of the droplets, the average speed of spreading increases slowly before reaching a plateau. The capillary length of the liquid ($L_c = \sqrt{\frac{\sigma}{\rho g}} \approx 2$ mm, where $\sigma = 41.2$ mN/m is the dynamic surface tension of the ALS 0.04 M) determines where the plateau starts. For the droplets with diameters smaller than the capillary length of the system, the average velocity grows linearly with the increasing radius of the droplet (slope 1 in the log−log plot of Figure 8b). After that, the speed remains constant at 0.5 ± 0.15 m/s. L_c is indicated in Figure 8b as a vertical dashed line. According to our results for the fast spreading, the volume of the spreading droplet does not affect the spreading exponent but the spreading speed can be influenced by the droplet volume when the diameter of the droplet is smaller than the capillary length of the liquid.

For the slow spreading, although the power law exponents are significantly smaller than unity ($\alpha \approx 0.11$), we still are able to linearly fit the time evolution data of Figure 7 and estimate a spreading speed. The results are shown by square symbols in Figure 8b and indicate that the average spreading speed remains approximately constant with an increase in the volume of the droplet.

3.3. Scaling Arguments. Bringing two miscible liquids into contact with each other will generate a gradient of surface tension and induces a Marangoni-driven flow. The driving force in such flows is the tangential stress associated with gradients of surface tension at the interface which should be balanced by viscous stresses. Based on scaling the Marangoni stresses for viscosity-limited spreading on a deep bath (distance as a function of time), a spreading exponent of 3/4 can be derived.[29−31]

The Reynolds number ($Re = \rho u h/\eta$, with h as the film thickness) of the system in the rapid spreading regime ($\Delta \sigma > 0$) is always larger than one, indicating that the inertial terms should be considered in the balance of stresses. In the first approximation, we ignore the viscous dissipation and balance the surface tension gradient by the inertial term: $|\nabla \sigma| \approx \rho u^2$, where $u \approx \dot{R}$ with a dot denoting the time derivative. The surface tension gradient term scales with the dynamic surface tension difference divided by the radius of the spreading front ($|\nabla \sigma| \approx \Delta \sigma/R$), so we arrive at $\Delta \sigma/R \approx \rho \dot{R}^2$ and hence, $R \approx (\Delta \sigma/\rho)^{1/3} t^{2/3}$. The exponent 2/3 is within the range of

exponents we observed for the fast spreading experiments, as shown in Figure 5a by a dashed line marked by "inertial".

4. CONCLUSIONS

Droplets will spread when deposited on a soap film. Spreading evolves as a function of time in a power-law manner with exponents ranging from about 0.1 to about 1 depending on the dynamic surface tension differences between the film and the droplet. Small spreading exponents with slow spreading dynamics occur when the surface tension of the droplet is greater than or equal to the surface tension of the film so that the tension difference does not favor spreading. This slow spreading regime resembles Tanner's spreading on a solid substrate with exponent 0.1, as driven by capillary pressure at the rim. By increasing the surface tension difference, the spreading exponent increases toward 1. In this regime, the spreading speed increases significantly with surface tension difference. Here, the driving mechanism is the Marangoni stress. By scaling the Marangoni stress with inertial terms, we can derive spreading exponents of $\alpha = 2/3$. Although this exponent is in the range of experimentally observed exponents for the fast spreading regime, however it does not explain the very fast spreading dynamics with exponents about one. This might be because of the fact that in our scaling argument, we have simplified all the kinetic effects and surfactant absorption dynamics in a surface tension gradient. We also find that the spreading speed depends on the size of the droplet in the fast spreading regime. The spreading speed depends linearly on the droplet size for drops smaller than the capillary length of the liquid and remains constant for larger droplet sizes; however, the spreading exponent is not influenced by the droplet size. Our experimental results may help in understanding of the various forces acting on a droplet deposited on a liquid interface. Using a more detailed theoretical model in which the surfactant absorption kinetics is considered may elucidate all our experimental observations. In addition, our methodology can be used for stretching complex liquid droplets in 2D and therefore may have applications in modifying thin suspended films. For example, using this approach, the effect of elongational viscosity on stretching a complex liquid droplet in 2D can be studied.

■ ASSOCIATED CONTENT

⑤ Supporting Information

The Supporting Information is available free of charge on the ACS Publications website at DOI: 10.1021/acs.langmuir.9b02274.

　　Dynamic surface tension measurements and determination of soap film thickness (PDF)

■ AUTHOR INFORMATION

Corresponding Author

*E-mail: mehdi.habibi@wur.nl.

ORCID ⊙

H. A. Stone: 0000-0002-9670-0639

D. Bonn: 0000-0001-8925-1997

Mehdi Habibi: 0000-0003-4672-0516

Author Contributions

R.S. observed this phenomenon for the first time. M.E., M.S., and R.S. performed preliminary experiments that are not reported here. R.S., E.v.d.L., D.B., H.A.S., M.M., and M.H. contributed in designing the research and the interpretation of the data. M.M. performed all the experiments and data analysis of this paper. M.M., M.H., and H.A.S. developed the theoretical models. M.M. and M.H. wrote the manuscript. All the authors reviewed and commented on the manuscript and discussed the results and models.

Notes

The authors declare no competing financial interest.

■ ACKNOWLEDGMENTS

■ REFERENCES

(1) Bonn, D.; Eggers, J.; Indekeu, J.; Meunier, J.; Rolley, E. Wetting and spreading. *Rev. Mod. Phys.* **2009**, *81*, 739−805.

(2) Carrier, O.; Bonn, D.; Brutin, D. Liquid Spreading. *Droplet Wetting and Evaporation*; Academic Press: Oxford, 2015; Chapter 1, pp 3−13.

(3) Buguin, A.; Chen, Y.; Silberzan, P. Microfluidics: Concepts and applications to the life sciences. *Nanoscience: Nanobiotechnology and Nanobiology*; Springer Berlin Heidelberg: Berlin, Heidelberg, 2009; pp 743−774.

(4) Bergeron, V.; Bonn, D.; Martin, J. Y.; Vovelle, L. Controlling droplet deposition with polymer additives. *Nature* **2000**, *405*, 772.

(5) Javadi, A.; Habibi, M.; Taheri, F. S.; Moulinet, S.; Bonn, D. Effect of wetting on capillary pumping in microchannels. *Sci. Rep.* **2013**, *3*, 1412.

(6) de Gennes, P. G. Wetting: statics and dynamics. *Rev. Mod. Phys.* **1985**, *57*, 827−863.

(7) Popescu, M. N.; Oshanin, G.; Dietrich, S.; Cazabat, A.-M. Precursor films in wetting phenomena. *J. Phys.: Condens. Matter* **2012**, *24*, 243102.

(8) Cazabat, A. M.; Gerdes, S.; Valignat, M. P.; Villette, S. Dynamics of wetting: from theory to experiment. *Interface Sci.* **1997**, *5*, 129−139.

(9) Fraaije, J. G. E. M.; Cazabat, A. M. Dynamics of spreading on a liquid substrate. *J. Colloid Interface Sci.* **1989**, *133*, 452−460.

(10) van Capelleveen, B. F.; Koldeweij, R.; Lohse, D.; Visser, C. W. On the universality of Marangoni-driven spreading along liquid-liquid interfaces. arXive:1712.03192, **2017**.

(11) Rafaï, S.; Bonn, D. Spreading of non-Newtonian fluids and surfactant solutions on solid surfaces. *Phys. A* **2005**, *358*, 58−67.

(12) Santiago-Rosanne, M.; Vignes-Adler, M.; Velarde, M. G. On the spreading of partially miscible liquids. *J. Colloid Interface Sci.* **2001**, *234*, 375−383.

(13) Camp, D. W.; Berg, J. C. The spreading of oil on water in the surface-tension regime. *J. Fluid Mech.* **1987**, *184*, 445−462.

(14) Wang, X.; Bonaccurso, E.; Venzmer, J.; Garoff, S. Deposition of drops containing surfactants on liquid pools: Movement of the contact line, Marangoni ridge, capillary waves and interfacial particles. *Colloids Surf., A* **2015**, *486*, 53−59.

(15) Afsar-Siddiqui, A. B.; Luckham, P. F.; Matar, O. K. The spreading of surfactant solutions on thin liquid films. *Adv. Colloid Interface Sci.* **2003**, *106*, 183−236.

(16) Tanner, L. H. The spreading of silicone oil drops on horizontal surfaces. *J. Phys. D: Appl. Phys.* **1979**, *12*, 1473.

(17) Cazabat, A. M.; Stuart, M. A. C. Dynamics of wetting: effects of surface roughness. *J. Phys. Chem.* **1986**, *90*, 5845−5849.

(18) Shiri, R.; Najafi, A.; Habibi, M. Sampling Moiré technique and the dynamics of a spreading droplet on a solid surface. *Meas. Sci. Technol.* **2014**, *25*, 035305.

(19) Hernández-Sánchez, J. F.; Eddi, A.; Snoeijer, J. H. Marangoni spreading due to a localized alcohol supply on a thin water film. *Phys. Fluids* **2015**, *27*, 032003.

(20) Jensen, O. E.; Grotberg, J. B. Insoluble surfactant spreading on a thin viscous film: shock evolution and film rupture. *J. Fluid Mech.* **1992**, *240*, 259−288.

(21) Gaver, D. P.; Grotberg, J. B. The dynamics of a localized surfactant on a thin film. *J. Fluid Mech.* **1990**, *213*, 127−148.

(22) Kang, K.-H.; Kim, H.-U.; Lim, K.-H. Effect of temperature on critical micelle concentration and thermodynamic potentials of micellization of anionic ammonium dodecyl sulfate and cationic octadecyl trimethyl ammonium chloride. *Colloids Surf., A* **2001**, *189*, 113−121.

(23) Mysels, P. M. a. K. J. Critical micelle concentrations of aqueous surfactant systems. *J. Pharm. Sci.* **1972**, *61*, 319.

(24) Price, H. C.; Mattsson, J.; Murray, B. J. Sucrose diffusion in aqueous solution. *Phys. Chem. Chem. Phys.* **2016**, *18*, 19207−19216.

(25) Joos, P.; Pintens, J. Spreading kinetics of liquids on liquids. *J. Colloid Interface Sci.* **1977**, *60*, 507−513.

(26) Aarts, D. G. A. L.; Lekkerkerker, H. N. W.; Guo, H.; Wegdam, G. H.; Bonn, D. Hydrodynamics of Droplet Coalescence. *Phys. Rev. Lett.* **2005**, *95*, 164503.

(27) Howell, P. D.; Stone, H. A. On the absence of marginal pinching in thin free films. *Eur. J. Appl. Math.* **2005**, *16*, 569−582.

(28) Rafaï, S.; Sarker, D.; Bergeron, V.; Meunier, J.; Bonn, D. Superspreading: aqueous surfactant drops spreading on hydrophobic surfaces. *Langmuir* **2002**, *18*, 10486−10488.

(29) Fay, J. A. Physical processes in the spread of oil on a water surface. *Int. Oil Spill Conf. Proc.* **1971**, *1971*, 463−467.

(30) Hoult, D. P. Oil Spreading on the Sea. *Annu. Rev. Fluid Mech.* **1972**, *4*, 341−368.

(31) Dussaud, A. D.; Troian, S. M.; Harris, S. R. Fluorescence visualization of a convective instability which modulates the spreading of volatile surface films. *Phys. Fluids* **1998**, *10*, 1588−1596.